BMC Medical Imaging

RESEARCH Open Access

The value evaluation of Nomogram prediction model based on CTA imaging features for selecting treatment methods for isolated superior mesenteric artery dissection

Xiaodong Jiang[1], Dongjian Chen[1], Qingbin Meng[1], Xiaokan Liu[1], Li Liang[1], Bosheng He[2*] and Wenbin Ding[1*]

Abstract

Objective To evaluate value of Nomogram prediction model based on CTA imaging features for selecting treatment methods for isolated superior mesenteric artery dissection (ISMAD).

Methods Symptomatic ISMAD patients were randomly divided into a training set and a validation set in a 7:3 ratio. In the training set, relevant risk factors for conservative treatment failure in ISMAD patients were analyzed, and a Nomogram prediction model for treatment outcome of ISMAD was constructed with risk factors. The predictive value of the model was evaluated.

Results Low true lumen residual ratio (TLRR), long dissection length, and large arterial angle (superior mesenteric artery [SMA]/abdominal aorta [AA]) were identified as independent high-risk factors for conservative treatment failure ($P < 0.05$). The receiver operating characteristic curve (ROC) results showed that the area under curve (AUC) of Nomogram prediction model was 0.826 (95% CI: 0.740–0.912), indicating good discrimination. The Hosmer-Lemeshow goodness-of-fit test showed good consistency between the predicted curve and the ideal curve of the Nomogram prediction model. The decision curve analysis (DCA) analysis results showed that when probability threshold for the occurrence of conservative treatment failure predicted was 0.05–0.98, patients could obtain more net benefits. Similar results were obtained for the predictive value in the validation set.

Conclusion Low TLRR, long dissection length, and large arterial angle (SMA/AA) are independent high-risk factors for conservative treatment failure in ISMAD. The Nomogram model constructed with independent high-risk factors has good clinical effectiveness in predicting the failure.

Keywords Isolated superior mesenteric artery dissection, CTA, Risk factors, Nomogram prediction model, Conservative medical treatment

*Correspondence:
Bosheng He
boshenghe@126.com
Wenbin Ding
drdwb@126.com

[1]Department of Interventional Radiology, Second Affiliated Hospital of Nantong University, No.666 Shengli Road, Nantong, Jiangsu 226014, Jiangsu, China
[2]Department of Department of Imaging Medicine, Second Affiliated Hospital of Nantong University, Nantong 226014, Jiangsu, China

Introduction

Predictive factors and classification models play a crucial role in the field of biomedical signal processing, effectively enhancing the accuracy of disease diagnosis and the customization of treatment plans. In the realm of drug discovery, these tools expedite the process of new drug development and increase success rates by identifying specific characteristics of potential drug molecules [1–5]. Classification models in medical image analysis help identify and categorize diseases or conditions based on images, while predictor models estimate outcomes or progression of these conditions, aiding in diagnosis and treatment planning [6–11].

With the rapid development of imaging technology, the number of reported cases of isolated superior mesenteric artery dissection (ISMAD) is increasing, especially in Asia [12–14]. The clinical manifestations of ISMAD range from asymptomatic to acute abdominal pain accompanied by intestinal ischemia or peritonitis. Although not as urgent as other mesenteric artery diseases, it can still potentially lead to severe mesenteric ischemia. It is currently believed that the etiology of ISMAD seems to be multifactorial and related to anatomical, genetic, and systemic factors. Regarding clinical manifestations and diagnosis, ISMAD has diverse and elusive clinical presentations. A significant number of ISMAD patients are asymptomatic and incidentally discovered [15]. Symptomatic patients typically present with localized abdominal pain in the upper abdomen, left flank, or umbilical region, which can be acute or chronic postprandial pain [16, 17]. It may also be associated with nausea, vomiting, rectal bleeding, diarrhea, or back pain. These nonspecific symptoms often delay the diagnosis of ISMAD, putting patients at risk of life-threatening complications [17]. Currently, computed tomography angiography (CTA) is the preferred diagnostic method for ISMAD, with literature reporting a diagnostic confirmation rate of approximately 95% using CTA [18]. In addition, color Doppler ultrasound and digital subtraction angiography (DSA) are also used as diagnostic modalities. Many researchers have reported the results of predicting ISMAD using relevant imaging features, which are beneficial for researchers to develop predictive factors [19–25]. However, these studies have only explored the role of relevant imaging features in the diagnosis and treatment of ISMAD, and there has been no report on their predictive value for the failure of conservative treatment.

Currently, the epidemiology, etiology, mechanisms, clinical features, and imaging characteristics of ISMAD have not been fully studied, and there is a lack of large-scale prospective or retrospective studies. As a result, there is no consensus on the optimal treatment management strategy for ISMAD. Apart from emergency surgery, the current standard treatment for ISMAD is mainly conservative medical treatment. Although conservative treatment has a high efficacy rate, there are still some patients who fail conservative treatment and subsequently require endovascular or surgical intervention [17]. Patients who fail conservative medical treatment usually require active intervention. Currently, the reasons why some ISMAD patients fail conservative treatment are still unclear. For this group of patients who fail conservative medical treatment, it is worth exploring whether invasive intervention measures can be chosen directly instead of conservative treatment to promote patient recovery and improve their quality of life. This is an important topic that deserves further investigation. CTA is the preferred diagnostic method for ISMAD and an important basis for its classification. Can predictive models related to ISMAD treatment outcomes be constructed based on the imaging characteristics obtained from CTA examinations or in combination with other indicators? Currently, there are few reports on this topic both domestically and internationally. In this study, symptomatic ISMAD patients were randomly divided into a training set and a validation set in a 7:3 ratio. In the training set, relevant risk factors for conservative treatment failure in ISMAD patients were analyzed, and a Nomogram prediction model for treatment outcome of ISMAD was constructed with risk factors. The predictive value of the model was evaluated. Through this study, we aims to ① explore the predictive value of CTA-related imaging characteristics in guiding the outcome of conservative medical treatment for ISMAD, ② provide theoretical evidence for the selection of treatment strategies for ISMAD.

The remainder of this paper is organized as follows: Methods outlines the study design, patient criteria, data collection, and statistical analysis for the Nomogram model. Results present key findings from the training and validation sets, including risk factors and model performance. Discussion compares results with prior studies, evaluates clinical significance, and notes limitations. Conclusion highlights key risk factors and the Nomogram model's practical use in ISMAD treatment decisions.

Methods

Patients

The Ethics Committee of Second Affiliated Hospital of Nantong University approved the study and informed consent to participate was waived (2022YKY040). The retrospective collection of symptomatic ISMAD patients who received conservative medical treatment at our center from July 2013 to July 2023 was the focus of this study. Failure of conservative medical treatment refers to the lack of symptom and sign relief or even aggravation, progression of imaging findings (such as continuous

extension of dissection or enlargement of false lumen), and the occurrence of intestinal necrosis or rupture of SMA during the course of conservative medical treatment [26]. The study population was divided into a success group and a failure group based on whether they experienced failure of conservative medical treatment. Inclusion criteria were as follows: ① Symptomatic ISMAD patients diagnosed by CTA; ② ISMAD patients who initially received conservative medical treatment upon admission; ③ Complete clinical baseline information; ④ Complete CTA imaging data. Exclusion criteria were as follows: ① Presence of other arterial dissections; ② Endovascular or surgical treatment as the preferred initial treatment; ③ Systemic vasculitis or other autoimmune diseases; ④ Insufficient image quality or inadequate clinical records.

Clinical baseline data

General information: Gender, age (years), body mass index (BMI), alcohol history, smoking history; Past medical history: History of hypertension, history of diabetes, history of abdominal surgery; Hematobiochemical indicators: Lymphocytes (10^9/L), platelets (10^9/L), Lactate dehydrogenase (U/L), procalcitonin (ng/ml), erythrocyte sedimentation rate (ESR) (/h), white blood cells (10^9/L), neutrophils (10^9/L), D-dimer (ug/L), fasting plasma glucose (FPG) (mmol/L), C-reactive protein (CRP) (mg/L), triglycerides (TG) (mmol/L), total cholesterol (TC) (mmol/L), low-density lipoprotein (LDL) (mmol/L), high-density lipoprotein (HDL) (mmol/L); Clinical manifestations: Lower back pain, nausea and vomiting, abdominal pain.

CTA imaging data

CTA imaging reconstruction: Performed using soft tissue convolution kernel (B25f Siemens) and iterative reconstruction technique (ADMIRE Siemens, strength level 3). Images processed with 1.0 mm slice thickness and 0.7 mm interval.

Post-processing: Transferred to Siemens Syngo.via workstation (version 30 A) for multi-planar reconstruction (MPR) and curved intensity projection (CPR) with 2 mm slice thickness and interval.

Observation indicators

① YUN classification [18]: Type I refers to a false lumen with inlet and outlet and unobstructed blood flow; Type IIa refers to a false lumen with inlet but no outlet; Type IIb refers to a false lumen with thrombus formation and no blood flow; Type III refers to both true and false lumens being completely blocked (Fig. 1a).

② True lumen residual ratio (TLRR): Ratio of the diameter of the true lumen to the proximal normal SMA lumen diameter [27] (Fig. 1b).

③ Dissection length: Measured on CPR, starting from the proximal end of the dissection to the distal end, measuring the length of the dissection (Fig. 1c).

④ Distance from the start of the dissection to the abdominal aorta (AA) (Fig. 1c).

⑤ SMA/AA angle: Angle measured between the long axes of the superior mesenteric artery (SMA) and abdominal aorta (AA). (Fig. 1c).

⑥ Dissecting aneurysm.

⑦ Involvement of branch vessels.

⑧ Intestinal ischemia.

⑨ Perivascular fat infiltration: Increased density and blurring of the fat around the SMA wall.

⑩ Riolan's arch.

Statistics processing

The 195 samples were randomly divided into a training set (136 cases) and a validation set (59 cases) in a 7:3 ratio. Measurement data from clinical baseline information and CTA imaging data were tested for normal distribution using the Kolmogorov-Smirnov D test. Data that followed a normal distribution were expressed as mean±standard deviation (mean±SD), and independent sample t-tests were used for between-group comparisons. Measurement data that did not follow a normal distribution were expressed as median (interquartile range), and the Mann-Whitney U test was used for between-group comparisons. Count data were expressed as number (percentage), and chi-square test or Fisher's exact test was used for between-group comparisons. A binary logistic regression was used to analyze the risk factors associated with conservative treatment failure in the training set. The identified independent high-risk factors for conservative treatment failure in the training set were used to build a Nomogram predictive model using logistic regression. The clinical effectiveness of the Nomogram predictive model was evaluated using receiver operating characteristic curve (ROC), Hosmer-Lemeshow goodness-of-fit test, calibration curves, and decision curve analysis (DCA).

The above-mentioned between-group differences in baseline analysis were conducted using SPSS 22.0 statistical software. ROC analysis was performed using MedCalc 18.2.1 statistical software. Risk factor analysis, predictive model construction and evaluation, SHAP analysis were conducted using R language R 4.2.3 statistical software, along with Zstats v0.90 (www.medsta.cn/software). A significance level of $P<0.05$ was considered statistically significant.

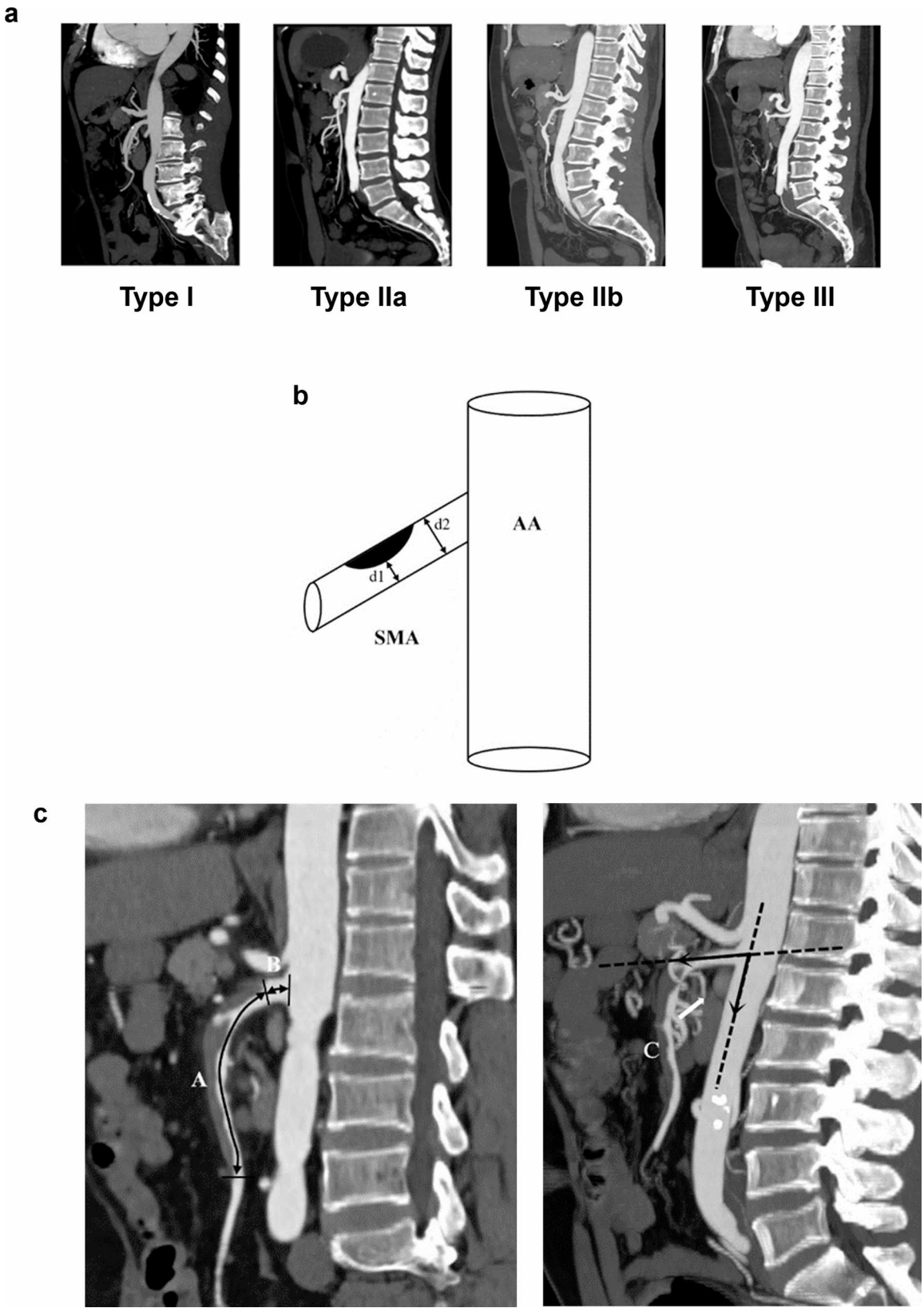

Fig. 1 Observation indicators in CTA imaging. **(a)** YUN classification. **(b)** TLRR = d1/d2 × 100%. **(c)** **A**: Dissection length; **B**: Distance from the start of the dissection to the AA; **C**: Angle between SMA and AA

Results

Baseline data comparison

Divided the 195 samples into a training set of 136 cases and a validation set of 59 cases according to a ratio of 7:3. The comparison of baseline data between the training set and validation set showed no significant difference between groups ($P>0.05$) (Table-1).

Screening of risk factors for conservative treatment failure

From the univariate results, it can be inferred that low TLRR, long length of the dissection, and large arterial angle (SMA/AA) are significant risk factors associated with conservative treatment failure ($P<0.05$) (Table-2). Multivariate results show that low TLRR, long length of the dissection, and large arterial angle (SMA/AA) are independent high-risk factors for conservative treatment failure ($P<0.05$) (Table-3).

The clinical value evaluation of Nomogram prediction model in the training set

According to the logistic regression analysis results, Nomogram prediction model was constructed with independent high-risk factors TLRR, dissection length, and angle (SMA/AA). The equation is as follows: Logit (P) = 0.034× Dissection length −1.807× TLRR + 0.021× Angle −4.193. The constructed prediction model was visualized using Nomogram (Fig. 2a).

The ROC results showed that the AUC of the prediction model was 0.826 (95%CI: 0.740–0.912) (Z = 7.405, $P<0.01$). The Nomogram prediction model demonstrated good discrimination, and its AUC was higher than that of TLRR, dissection length, and angle (SMA/AA) when predicted separately (Table-4; Fig. 2b).

The Hosmer-Lemeshow goodness-of-fit test result showed that $\chi2=7.47$, $P=0.49$, $P>0.05$. The calibration curve showed good consistency between the predicted curve and the ideal curve in the Nomogram prediction model (Fig. 2c).

The DCA results showed that when the probability threshold for predicting conservative treatment failure using the Nomogram model ranged from 0.05 to 0.98, patients could obtain a greater net benefit. Additionally, the area under the curve was large, indicating that the model is suitable for clinical application (Fig. 2d).

Nomogram predictive model's clinical effectiveness verification in validation set

The ROC results of the validation dataset showed that the AUC of the predictive model was 0.903 (95% CI: 0.828–0.979) (Z = 10.458, $P<0.01$). The Nomogram predictive model also demonstrates good predictive performance in the validation set (Table-5; Fig. 3a).

The results of the Horsmer-Lemeshow goodness-of-fit test show that $\chi2=6.20$, $P=0.63$, and the calibration curve assessment showed a good fit between the predicted curve and the ideal curve, indicating that the prediction model also performs well in the validation set (Fig. 3b).

The DCA analysis results showed that when the probability threshold for predicting conservative treatment failure in the validation set was set between 0.05 and 0.90, patients could also benefit more from the model and had a larger area under the curve, which was suitable for clinical application (Fig. 3c).

The SHAP to model interpretation

To visually explain the selected variables, we used SHAP to illustrate how these variables predicted conservative treatment failure in the model. Fig. 4a shows the three most important features in our model. In each feature important line, the attributions of all patients to the results are plotted with different colored dots, where orange dots represent high risk values and purple dots represent low risk values. Low TLRR, long dissection length, and large arterial angle (SMA/AA) would elevate conservative treatment failure in ISMAD. Simultaneous display the ranking of risk factors evaluated by the average absolute SHAP value, with the x-axis SHAP value indicating the importance of the forecast model. In addition, we provided two typical examples to illustrate the interpretability of the model, one was a patient without conservative treatment failure with a low SHAP predictive score (-0.211) (Fig. 4b), while another patient with conservative treatment failure had a higher SHAP score (0.528) (Fig. 4c).

Discussion

The main treatment methods for ISMAD currently include conservative medical treatment, endovascular intervention, and surgical operation [28–30]. The 2017 ESVS guidelines [31] recommend conservative treatment for patients without acute intestinal necrosis. Ye et al. [32] considered SISMAD a self-limiting disease, and conservative treatment as first-line therapy. Xu et al. [33] conducted long-term follow-up on 15 conservatively treated patients, with symptom relief rate of 93.3%. Jang et al. [34] retrospectively studied 54 patients with ISMAD over 3 years. All initially received conservative treatment, with average follow-up of 18.5 months. Seven underwent endovascular treatment due to worsening symptoms or aneurysm development, while the remainder were successfully managed conservatively, for a conservative success rate of 87%. In this study, of 19conservatively teatedpatients, 150 achieved good results(76.92%). Compared to previous literature reports, the conservative success rate was slightly lower; possibly due to inclusion of symptomatic patients only. Generally, conservative treatment for ISMAD can achieve good therapeutic effects. However, some patients may experience treatment

Table 1 Training set and validation set baseline data comparison

	Total (*n* = 195)	**Training set (*n* = 136)**	**Validation set (*n* = 59)**	**Statistical value**	***P***
Age	56.00 (50.50–63.00)	55.00 (50.00–63.00)	57.00 (51.00–64.50)	Z = 1.053	0.293
Gender				χ^2=0.004	0.951
male	169 (86.67)	118 (86.76)	51 (86.44)		
femal	26 (13.33)	18 (13.24)	8 (13.56)		
BMI	23.01 ± 3.15	22.83 ± 3.28	23.41 ± 2.84	t=-1.167	0.244
Smoking history				χ^2=0.114	0.735
no	142 (72.82)	100 (73.53)	42 (71.19)		
yes	53 (27.18)	36 (26.47)	17 (28.81)		
Drinking history				χ^2=0.029	0.866
no	173 (88.72)	121 (88.97)	52 (88.14)		
yes	22 (11.28)	15 (11.03)	7 (11.86)		
Hypertension history				χ^2=0.537	0.464
no	118 (60.51)	80 (58.82)	38 (64.41)		
yes	77 (39.49)	56 (41.18)	21 (35.59)		
Diabetes history				χ^2=0.038	0.846
no	179 (91.79)	124 (91.18)	55 (93.22)		
yes	16 (8.21)	12 (8.82)	4 (6.78)		
Abdominal surgery history				χ^2=0.058	0.810
no	177 (90.77)	123 (90.44)	54 (91.53)		
yes	18 (9.23)	13 (9.56)	5 (8.47)		
Lymphocytes (10^9/L)	2.45 ± 0.97	2.47 ± 0.98	2.41 ± 0.94	t = 0.389	0.698
Platelets (10^9/L)	204.40 ± 62.83	203.98 ± 63.39	205.37 ± 62.04	t=-0.142	0.887
Lactate dehydrogenase (U/L)	213.01 ± 63.58	213.35 ± 63.83	212.20 ± 63.56	t = 0.116	0.908
procalcitonin (ng/ml)	0.07 ± 0.21	0.05 ± 0.01	0.13 ± 0.39	t=-1.494	0.141
ESR (/h)	15.22 ± 6.46	15.29 ± 6.64	15.07 ± 6.08	t = 0.217	0.828
White blood cells (10^9/L)	7.00 (5.35–9.50)	6.95 (5.38–9.50)	7.20 (5.20–9.30)	Z = 0.048	0.961
Neutrophils (10^9/L)	5.30 (3.80–7.85)	5.25 (3.70–7.80)	5.30 (4.10–8.05)	Z = 0.325	0.745
D-dimer (ug/L)	470.00 (219.00–970.00)	456.00 (219.50–962.00)	520.00 (220.00–996.00)	Z=-0.267	0.790
FPG (mmol/L)	5.52 (4.88–6.42)	5.61 (4.95–6.44)	5.42 (4.83–6.20)	Z = 1.003	0.316
CRP (mg/L)	7.62 (3.51–10.86)	7.49 (3.74–10.93)	8.39 (3.51–10.62)	Z = 0.160	0.873
TG (mmol/L)	1.63 (0.94–2.26)	1.60 (0.97–2.25)	1.64 (0.79–2.29)	Z = 0.421	0.674
TC (mmol/L)	4.11 ± 1.06	4.17 ± 1.13	3.97 ± 0.84	t = 1.376	0.171
LDL (mmol/L)	2.62 ± 0.73	2.65 ± 0.74	2.55 ± 0.73	t = 0.853	0.395
HDL (mmol/L)	1.33 (1.07–1.56)	1.31 (1.07–1.52)	1.40 (1.10–1.60)	Z = 0.884	0.377
Abdominal pain				χ^2=0.000	1.000
no	7(3.59)	5(3.68)	2(3.39)		
yes	188(96.41)	131(96.32)	57(96.61)		
Lower back pain				χ^2=0.015	0.901
no	171 (87.69)	119 (87.50)	52 (88.14)		
yes	24 (12.31)	17 (12.50)	7 (11.86)		
nausea and vomiting				χ^2=0.082	0.774
no	163 (83.59)	113 (83.09)	50 (84.75)		
yes	32 (16.41)	23 (16.91)	9 (15.25)		
TLRR	0.50 (0.21–0.79)	0.50 (0.28–0.79)	0.37 (0.18–0.65)	Z = 1.542	0.123
Dissection length	50.00 (36.00–72.00)	48.50 (36.00–70.50)	52.00 (40.00–75.50)	Z = 1.155	0.248
Distance from the start of the dissection to the AA	11.96 ± 5.45	11.85 ± 5.46	12.24 ± 5.48	t=-0.460	0.646
arterial angle (SMA/AA)	72.00 (45.50–88.50)	71.00 (45.00–88.25)	72.00 (47.50–89.00)	Z = 0.579	0.563
YUN classification				-	0.729
I	14 (7.18)	8 (5.88)	6 (10.17)		
IIa	70 (35.9)	50 (36.76)	20 (33.90)		
IIIb	96 (49.23)	67 (49.26)	29 (49.15)		
IV	15 (7.69)	11 (8.09)	4 (6.78)		

Table 1 (continued)

	Total (*n* = 195)	Training set (*n* = 136)	Validation set (*n* = 59)	Statistical value	*P*
Dissecting aneurysm				χ^2=2.470	0.116
no	144 (73.85)	96 (70.59)	48 (81.36)		
yes	51 (26.15)	40 (29.41)	11 (18.64)		
Involvement of branch vessels				χ^2=2.627	0.105
no	144 (73.85)	105 (77.21)	39 (66.10)		
yes	51 (26.15)	31 (22.79)	20 (33.90)		
Intestinal ischemia				-	1.000
no	192 (98.46)	134 (98.53)	58 (98.31)		
yes	3 (1.54)	2 (1.47)	1 (1.69)		
Perivascular fat infiltration				χ^2=2.409	0.121
no	128 (65.64)	94 (69.12)	34 (57.63)		
yes	67 (34.36)	42 (30.88)	25 (42.37)		
Riolan's arch				χ^2=1.029	0.310
no	164 (84.1)	112 (82.35)	52 (88.14)		
yes	31 (15.9)	24 (17.65)	7 (11.86)		

Note: AA: abdominal aorta; body mass index (BMI); CRP: C-reactive protein; ESR: erythrocyte sedimentation rate; FPG: fasting plasma glucose; HDL: high-density lipoprotein; LDL: low-density lipoprotein; SMA: superior mesenteric artery; TC: total cholesterol; TG: triglycerides; TLRR: True lumen residual ratio

Table 2 Single factor binomial logistic regression analysis of risk factors associated with conservative treatment failure

	β	S.E	Z	OR (95%CI)	*P* value
TLRR	-2.85	0.83	-3.43	0.06 (0.01–0.29)	**< 0.001**
Dissection length	0.04	0.01	4.54	1.04 (1.02–1.06)	**< 0.001**
Arterial angle (SMA/AA)	0.02	0.01	2.49	1.02 (1.01–1.04)	**0.013**

Note: AA: abdominal aorta; SMA: superior mesenteric artery; TLRR: True lumen residual ratio

Table 3 Multiple factors binomial logistic regression analysis of independent risk factors associated with conservative treatment failure

	β	S.E	Z	OR (95%CI)	*P* value
TLRR	-1.81	0.90	-2.00	0.16 (0.03–0.96)	**0.045**
Dissection length	0.03	0.01	3.67	1.03 (1.02–1.05)	**< .001**
Arterial angle (SMA/AA)	0.02	0.01	2.12	1.02 (1.01–1.04)	**0.034**

Note: AA: abdominal aorta; SMA: superior mesenteric artery; TLRR: True lumen residual ratio

failure, manifesting as recurrent abdominal pain, dissection aneurysm development, rupture with bleeding, intestinal ischemic necrosis, or death. Repeat endovascular intervention or surgery may be needed but prognosis remains poor. The aim of this study is to use CTA imaging characteristics, combined with other indicators, to construct a predictive model for ISMAD treatment selection, enabling early intervention for unsuitable conservative patients and improving prognosis.

Our results indicated that low TLRR, long dissection length, and large arterial angle (SMA/AA) were risk factors associated with conservative treatment failure. Low TLRR, long dissection length, and large arterial angle (SMA/AA) were indentified as independent high-risk factors for conservative treatment failure. Chen et al. [35] suggested that severe true lumen stenosis is prone to conservative treatment failure.; our study found that low TLRR was an independent high-risk factor for conservative treatment failure, which is consistent with previous literature. Acute presentation is typical of ISMAD, and low TLRR (high stenosis rate) can lead to acute intestinal ischemia. However, the establishment of collateral circulation between the SMA and the inferior mesenteric artery or abdominal aorta takes time, so low TLRR may lead to intestinal necrosis, and increased likelihood of conservative failure. In our study, long dissection length was an independent high-risk factor for conservative treatment failure. Prolongation of the anatomical length of the dissection can slow blood flow velocity and increase the risk of true lumen stenosis, leading to intestinal ischemia. Therefore, patients with longer dissection length should be carefully observed and evaluated. Liu et al. [36] conducted a retrospective study finding the arterial angle (SMA/AA) is an independent predictive factor for ISMAD prognosis. Our study identified a large arterial angle (SMA/AA) as an independent high-risk factor for conservative treatment failure, consistent with previous research. This may be related to increased shear stress and increased ISMAD incidence with larger arterial angle. In conclusion, low TLRR, long dissection length, and large arterial angle (SMA/AA) are independent high-risk factors for conservative treatment failure.

Clinical prediction models should exhibit discrimination, consistency, and clinical effectiveness. We use ROC analysis to evaluate discrimination, Hosmer-Lemeshow goodness-of-fit test to assess consistency, and decision curve analysis (DCA) to evaluate clinical effectiveness. This study showed all three factors had some predictive value for conservative treatment failure. Based on logistic regression analysis results, a nomogram prediction

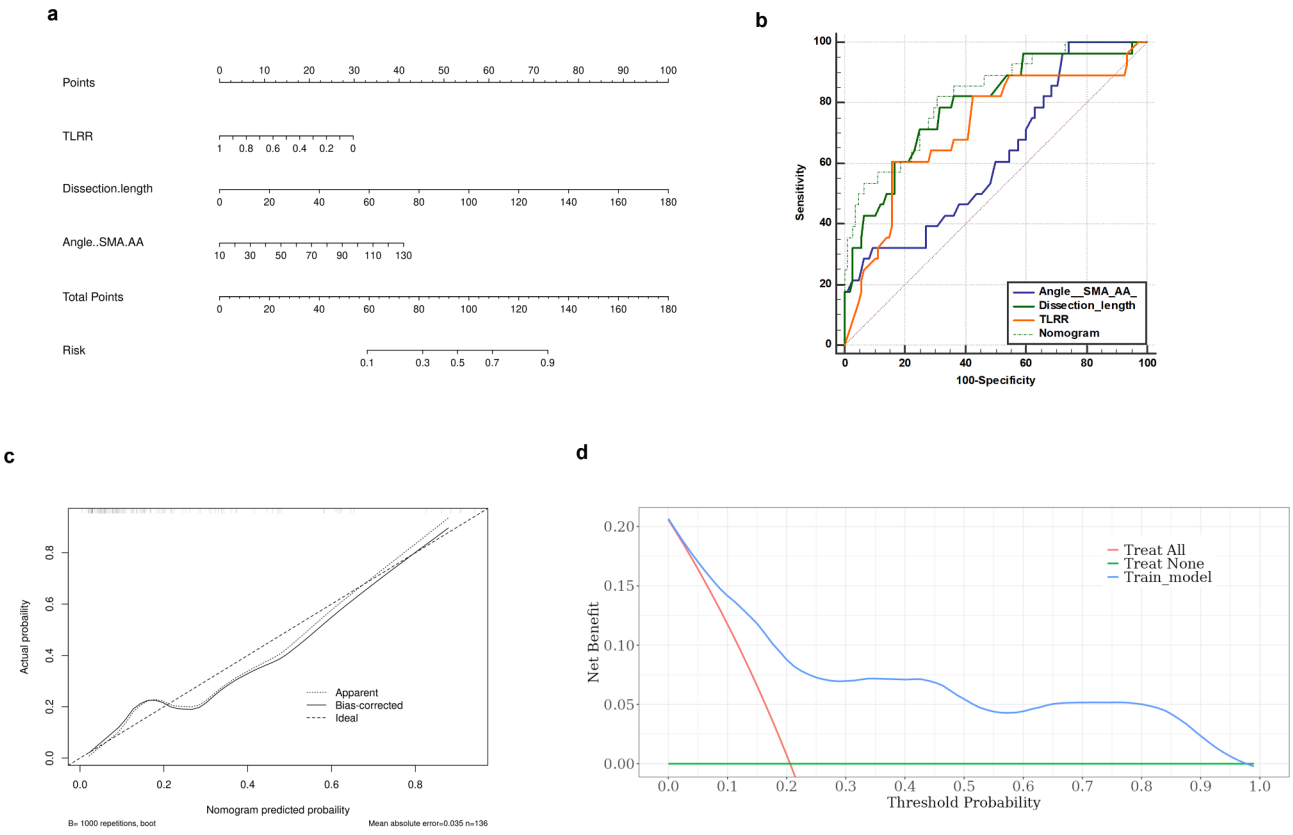

Fig. 2 The clinical value evaluation of Nomogram prediction model in the training set. **(a)** The constructed prediction model with independent risk factors was visualized using Nomogram. **(b)** The result of ROC. **(c)** The result of calibration curve. **(d)** The result of DCA

Table 4 ROC evaluated the performance of Nomogram prediction model in training set

	Youden index	Cutoff	AUC (95%CI)	Sensitivity (%)	Specificity (%)	Accuracy (%)
TLRR	0.500	0.26	0.719(0.605–0.833)	60.71	84.26	79.41
Dissection length	0.471	55	0.791(0.694–0.887)	78.57	68.52	70.59
Arterial angle (SMA/AA)	0.259	39	0.625(0.509–0.741)	100.00	25.93	41.18
Nomogram model	0.516	0.147	0.826(0.740–0.912)	82.14	69.44	72.06

Note: AA: abdominal aorta; AUC: area under curve; ROC: receiver operating characteristic curve; SMA: superior mesenteric artery; TLRR: True lumen residual ratio

Table 5 ROC evaluated the performance of Nomogram prediction model in validation set

	Youden index	Cutoff	AUC (95%CI)	Sensitivity (%)	Specificity (%)	Accuracy (%)
Nomogram model	0.740	0.353	0.903(0.828–0.979)	88.24	85.71	86.44

Note: AA: abdominal aorta; AUC: area under curve; ROC: receiver operating characteristic curve; SMA: superior mesenteric artery; TLRR: True lumen residual ratio

model was constructed using TLRR, dissection length, and arterial angle (SMA/AA). The ROC results indicated good discrimination for the nomogram prediction model, with a higher AUC compared to individual predicions using TLRR, dissection length, and arterial angle (SMA/AA). The prediction curve had a good fit with the ideal curve, indicating good consistency. DCA analysis showed patients could gain more net benefits when the probability threshold for the nomogram model predicting conservative treatment failure was between 0.00 and 0.99, with a large area under the curve, indicating good clinical effectiveness. Next, we evaluated the models generalization ability using the same methods on our validation set. The results showed consistent outcomes on the validation set as with the training set. The clinical effectiveness of the nomogram prediction model was also validated in the validation set. We applied the SHAP method to the prediction model to achieve the optimal predictive effect and interpretability. This study has some limitations. Firstly, it is a retrospective study with a relatively small sample sizes, and future prospective studies with a larger sample size and multiple centers should be conducted. Secondly, the predictive model constructed was not externally validated. Lastly, this study was a

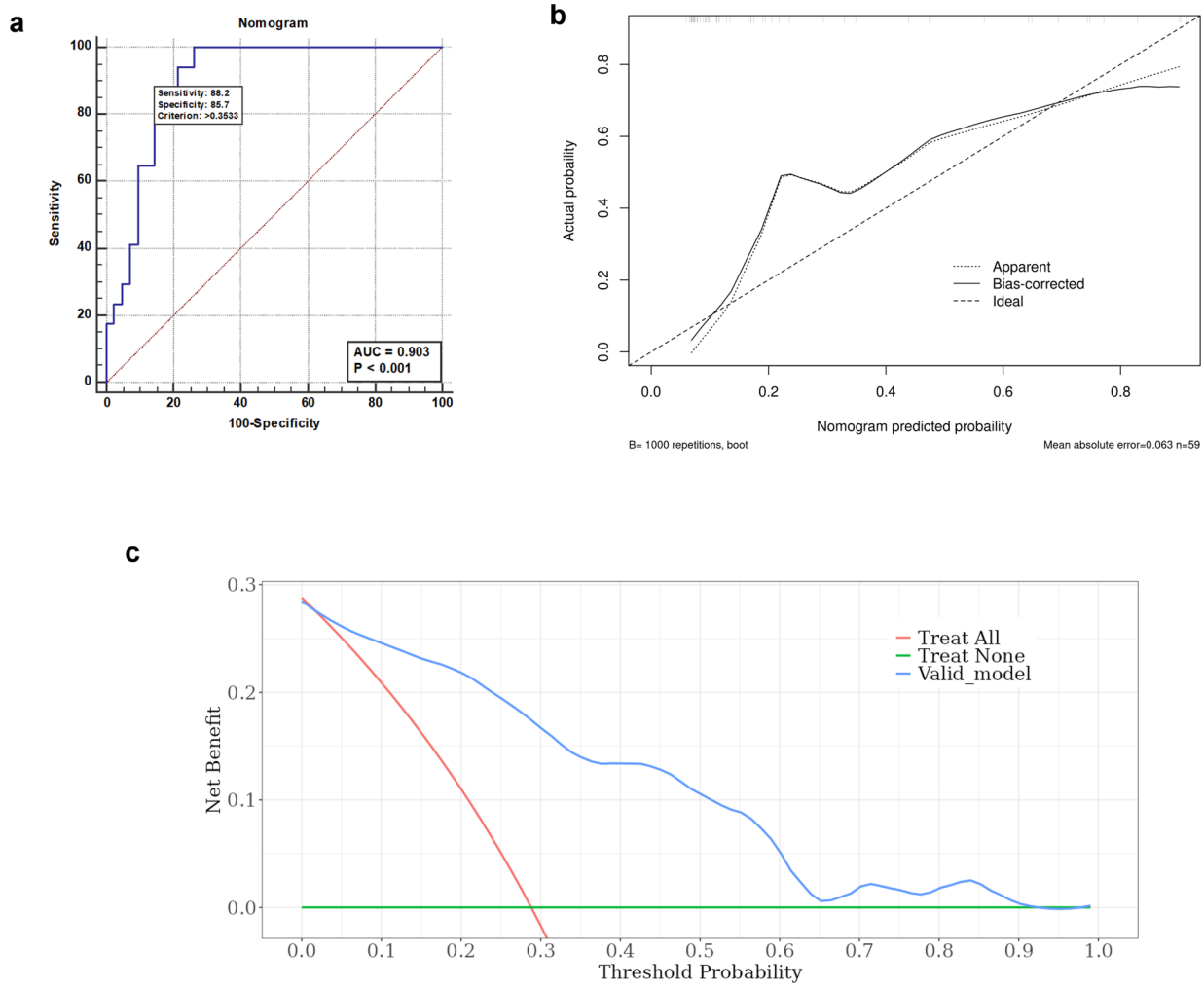

Fig. 3 Nomogram predictive model's clinical effectiveness verification in validation set. **(a)** The result of ROC. **(b)** The result of calibration curve. **(c)** The result of DCA

single-center study and may be subject to selection bias. Therefore, further in-depth research with larger sample sizes and multiple centers is needed for validation.

In summary, there are differences in CTA imaging findings between the successful and failed conservative treatment groups for symptomatic ISMAD. Low TLRR, long dissection length, and large arterial angle (SMA/AA) are independent high-risk factors for conservative treatment failure. The Nomogram model constructed based on these independent high-risk factors has good clinical effectiveness in predicting conservative treatment failure in ISMAD. Therefore, for patients meeting the criteria of the nomogram model, it is not recommended to undergo conservative treatment, but rather to directly consider invasive intervention measures. This approach can promote patient recovery and improve their quality of life.

Conclusion

Low TLRR, long dissection length, and large arterial angle (SMA/AA) are independent high-risk factors for conservative treatment failure in ISMAD. The Nomogram model constructed with independent high-risk factors has good clinical effectiveness in predicting the failure.

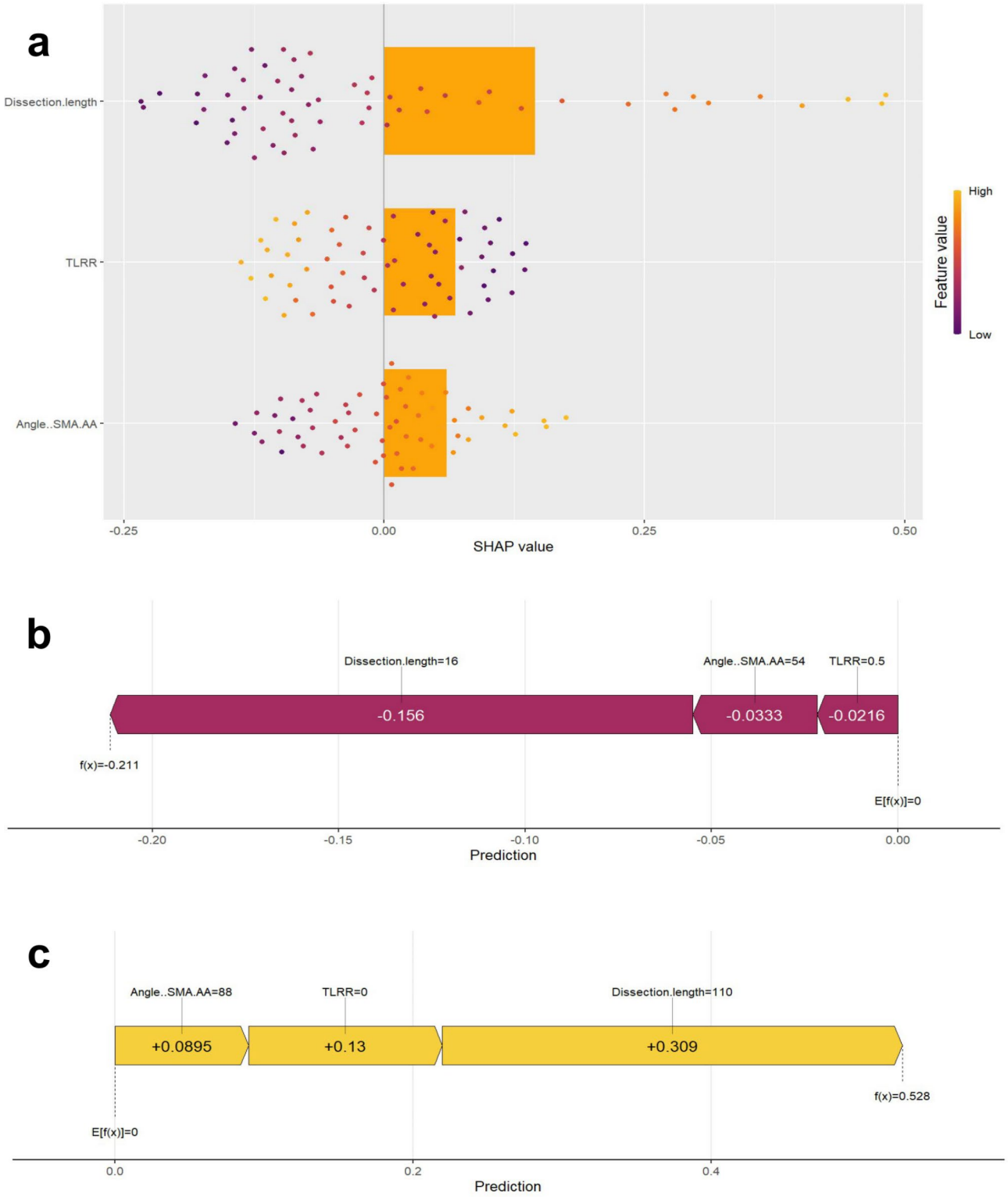

Fig. 4 SHAP interprets the model. **(a)** Attributes of characteristics in SHAP. **(b)** Individual efforts by patients without conservative treatment failure. **(c)** Individual efforts by patients with conservative treatment failure

Supplementary Information

The online version contains supplementary material available at https://doi.org/10.1186/s12880-024-01438-7.

Supplementary Material 1

Acknowledgements
None.

Author contributions
B.H. and W.D. conceived and designed the study. X.J., D.C., Q.M., X.L. and L.L. collected and analyzed the data. X.J. wrote the draft manuscript. BH revised the manuscript. All authors reviewed the manuscript.

Funding
None.

Data availability
Data supporting the findings of this study are available from the corresponding author upon reasonable request.

Declarations

Ethics approval and consent to participate
The Ethics Committee of Second Affiliated Hospital of Nantong University approved the study and informed consent to participate was waived (2022YKY040).

Consent for publication
N/A.

Competing interests
The authors declare no competing interests.

Received: 13 March 2024 / Accepted: 23 September 2024
Published online: 07 October 2024

References

1. Ansari MY, Qaraqe M, Charafeddine F, Serpedin E, Righetti R, Qaraqe K. Estimating age and gender from electrocardiogram signals: a comprehensive review of the past decade. Artif Intell Med. 2023;146:102690.
2. Ansari MY, Qaraqe M. MEFood: a large-scale Representative Benchmark of Quotidian Foods for the Middle East. IEEE Access. 2023;11:4589–601.
3. Ansari MY, Qaraqe M, Righetti R, Serpedin E, Qaraqe K. Enhancing ECG-based heart age: impact of acquisition parameters and generalization strategies for varying signal morphologies and corruptions. Front Cardiovasc Med 2024, 11.
4. Ansari MY, Chandrasekar V, Singh AV, Dakua SP. Re-routing drugs to blood brain barrier: a Comprehensive Analysis of Machine Learning approaches with fingerprint amalgamation and data balancing. IEEE Access. 2023;11:9890–906.
5. Chandrasekar V, Ansari MY, Singh AV, Uddin S, Prabhu KS, Dash S, Khodor SA, Terranegra A, Avella M, Dakua SP. Investigating the Use of Machine Learning models to understand the drugs permeability across Placenta. IEEE Access. 2023;11:52726–39.
6. Han Z, Jian M, Wang G-G. ConvUNeXt: an efficient convolution neural network for medical image segmentation. Knowl Based Syst 2022, 253.
7. Kunkyab T, Bahrami Z, Zhang H, Liu Z, Hyde D. A deep learning-based framework (Co-ReTr) for auto-segmentation of non-small cell-lung cancer in computed tomography images. J Appl Clin Med Phys. 2024;25(3):e14297.
8. Ansari MY, Abdalla A, Ansari MY, Ansari MI, Malluhi B, Mohanty S, Mishra S, Singh SS, Abinahed J, Al-Ansari A, et al. Practical utility of liver segmentation methods in clinical surgeries and interventions. BMC Med Imaging. 2022;22(1):97.
9. Rai P, Ansari MY, Warfa M, Al-Hamar H, Abinahed J, Barah A, Dakua SP, Balakrishnan S. Efficacy of fusion imaging for immediate post-ablation assessment of malignant liver neoplasms: a systematic review. Cancer Med. 2023;12(13):14225–51.
10. Ansari MY, Changaai Mangalote IA, Meher PK, Aboumarzouk O, Al-Ansari A, Halabi O, Dakua SP. Advancements in Deep Learning for B-Mode Ultrasound Segmentation: a Comprehensive Review. IEEE Trans Emerg Top Comput Intell. 2024;8(3):2126–49.
11. Ansari MY, Qaraqe M, Righetti R, Serpedin E, Qaraqe K. Unveiling the future of breast cancer assessment: a critical review on generative adversarial networks in elastography ultrasound. Front Oncol. 2023;13:1282536.
12. Kim H, Labropoulos N. The role of aortomesenteric angle in occurrence of spontaneous isolated superior mesenteric artery dissection. Int Angiol. 2020;39(2):125–30.
13. Jia Z, Su H, Chen W, Ni G, Qi C, Gu J. Endovascular treatment of patients with isolated mesenteric artery dissection aneurysm: Bare stents alone Versus Stent assisted coiling. Eur J Vasc Endovasc Surg. 2019;57(3):400–6.
14. Kimura Y, Kato T, Inoko M. Outcomes of treatment strategies for isolated spontaneous dissection of the Superior Mesenteric artery: a systematic review. Ann Vasc Surg. 2018;47:284–90.
15. DeCarlo C, Ganguli S, Borges JC, Schainfeld RM, Mintz AJ, Mintz J, Jaff MR, Weinberg I. Presentation, treatment, and outcomes in patients with spontaneous isolated celiac and superior mesenteric artery dissection. Vascular Med. 2017;22(6):505–11.
16. Daoud H, Abugroun A, Subahi A, Khalaf H. Isolated Superior Mesenteric Artery dissection: a Case Report and Literature Review. Gastroenterol Res. 2018;11(5):374–8.
17. Eldine RN, Dehaini H, Hoballah J, Haddad F. Isolated Superior Mesenteric Artery dissection: a Novel etiology and a review. Annals Vascular Dis. 2022;15(1):1–7.
18. Yun WS, Kim YW, Park KB, Cho SK, Do YS, Lee KB, Kim DI, Kim DK. Clinical and angiographic follow-up of spontaneous isolated Superior Mesenteric Artery Dissection. Eur J Vasc Endovasc Surg. 2009;37(5):572–7.
19. Dou L, Tang H, Zheng P, Wang C, Li D, Yang J. Isolated superior mesenteric artery dissection: CTA features and clinical relevance. Abdom Radiol (NY). 2020;45(9):2879–85.
20. Yoo J, Lee JB, Park HJ, Lee ES, Park SB, Kim YS, Choi BI. Classification of spontaneous isolated superior mesenteric artery dissection: correlation with multi-detector CT features and clinical presentation. Abdom Radiol (NY). 2018;43(11):3157–65.
21. Wu Z, Yi J, Xu H, Guo W, Wang L, Chen D, Xiong J. The significance of the Angle between Superior Mesenteric Artery and aorta in spontaneous isolated Superior Mesenteric Artery Dissection. Ann Vasc Surg. 2017;45:117–26.
22. Kimura Y, Kato T, Nagao K, Izumi T, Haruna T, Ueyama K, Inada T, Inoko M. Outcomes and Radiographic findings of isolated spontaneous Superior Mesenteric Artery Dissection. Eur J Vasc Endovasc Surg. 2017;53(2):276–81.
23. Ullah W, Mukhtar M, Abdullah HM, Ur Rashid M, Ahmad A, Hurairah A, Sarwar U, Figueredo VM. Diagnosis and management of isolated Superior Mesenteric Artery dissection: a systematic review and Meta-analysis. Korean Circ J. 2019;49(5):400–18.
24. Acosta S, Goncalves FB. Management of spontaneous isolated mesenteric artery dissection: a systematic review. Scand J Surg. 2021;110(2):130–8.
25. Eldine RN, Dehaini H, Hoballah J, Haddad F. Isolated Superior Mesenteric Artery dissection: a Novel etiology and a review. Ann Vasc Dis. 2022;15(1):1–7.
26. Peripheral Vascular Intervention Specialty Committee of the Interventional Radiology Branch CMDA. Expert Consensus on the diagnosis and treatment of isolated Superior Mesenteric Artery Dissection. Chin J Radiol. 2021;55(4):352–8.
27. Xu Y, Gao X, Shang D, Liu J, Jin B, Chen W. Outcomes and radiographic findings of symptomatic isolated mesenteric artery dissection with conservative management. Vascular. 2020;29(1):45–53.
28. Ben Abdallah I, Craiem D, Casciaro M, Deza D, Garzelli L, Nuzzo A, Corcos O, Ronot M, Castier Y, El Batti S. Volumetric analysis of progressive remodeling of isolated mesenteric artery dissection treated by conservative therapy. J Vasc Interv Radiol. 2023;34(3):445–53.
29. Wang CC, Sun YD, Wei XL, Jing ZP, Zhao ZQ. [Advances in the classification and treatment of isolated superior mesenteric artery dissection]. Zhonghua Wai Ke Za Zhi. 2023;61(1):81–5.
30. Qi X, Tang B, Zhang H, Fu J, Chen Y, Luo H. Midterm results of the conservative, Bare Stent, and Bare Stent-assisted coiling treatments for symptomatic isolated Superior Mesenteric Artery Dissection. Ann Vasc Surg 2023.
31. Bjorck M, Koelemay M, Acosta S, Bastos Goncalves F, Kolbel T, Kolkman JJ, Lees T, Lefevre JH, Menyhei G, Oderich G et al. Editor's Choice 2017 Management of the diseases of Mesenteric Arteries and veins: clinical practice guidelines of the European society of vascular surgery (ESVS). Eur J Vasc Endovasc Surg 53 4 460–510.

32. Ye M, Zhou Q, Wu J, Zhang Z, Li B, Zheng T, Shao G. Conservative Versus Endovascular treatment for spontaneous isolated Superior Mesenteric Artery Dissection: A Clinical and Imaging follow-up study. J Endovasc Ther 2023:15266028231163733.
33. Xu L, Shao J, Zhang D, Qiu C, Wang J, Li K, Fang L, Zhang X, Lei J, Lai Z, et al. Long-term outcomes of conservative treatment and endovascular treatment in patients with symptomatic spontaneous isolated superior mesenteric artery dissection: a single-center experience. BMC Cardiovasc Disord. 2020;20(1):256.
34. Jang JH, Cho BS, Ahn HY, Lee S, Kim H, Kim CN. Optimal treatment strategy and natural history of isolated Superior Mesenteric Artery Dissection based on Long-Term follow-up CT findings. Ann Vasc Surg. 2020;63:179–85.
35. Chen X, Xu L, Xu Z, Fan Z, Huang J, Li J, Zhang Z, Lin C. Analysis of safety and efficacy of conservative treatment and endovascular treatment in patients with spontaneous isolated mesenteric artery dissection. Front Surg. 2022;9:944079.
36. Guoqing L, Weicui C, Aihua O, Xia L, Liting M, Zelan M, Yun W. The value of CT plain scan signs in diagnosing spontaneous isolated superior mesenteric artery dissection. J Clin Radiol. 2022;41(6):1070–6.

Publisher's note